# SUPPLEMENTAL METHODS, FIGURES AND TABLES

Salina Nicoleau et al. 3D Modelling of Pulmonary Arterial Geometry and Endothelial Dysfunction in CTEPH



## SUPPLEMENTAL METHODS

**Segmentation of pulmonary arterial geometries**.

All segmentations were performed using Mimics 23.0 (Materialise, 2021). CTPA scans were imported as Digital Imaging and Communications in Medicine (DICOM) files. First, a mask was created to differentiate the cardiovascular components from bones and fat tissues. This was done by adjusting the Hounsfield Units threshold for the regions of interest (ROI). The mask was then split to isolate the pulmonary arteries from other structures, such as the ascending aorta and superior vena cava. The pulmonary artery mask was further refined and manually edited using the "multiple slice editor" and "mask editor" functions. The "smart filling" tool was used to unify the model and fill any gaps in the masks. In the presence of a contrast-filling defect due to an occluding thrombus, the defects were filled by following the outer lining of the arteries. 3D reconstructions of the pulmonary arteries were obtained through the "calculate parts" function. The 3D model was refined by further modifying the mask and smoothing the model's surface (5-10 iterations with a smoothing factor of 1 were used)

Pulmonary arterial diameters and lengths were measured by fitting a centerline through the reconstructed 3D vascular tree. The "best fit diameter" tool was used to measure the diameters at different points in the main, right and left pulmonary arteries; the average best fit diameter was taken across 3 points for each artery.

**Design of semi-circular channels.**

Fully circular and semi-circular channels recreating the ring-like stenoses and average dimensions observed in CTPA scans from CTEPH patients obtained from the Hammersmith Hospital (London, UK) and the literature (128,177,213,418–420) were designed in Fusion 360 (AutoDesk).

CTEPH patients included in this study (n=7) showed pulmonary arterial stenoses ranging from 20.84% to 84.81% (mean 47.52 ± 15.40%), while the degree of stenosis in CTEPH patients measured based on published data ranged from 37.3% to 85%. Obstructions were found mostly in the proximal pulmonary arteries, although they were also seen in other regions of the pulmonary arterial tree CT-scan and literature-derived measurements of pulmonary arterial stenosis are summarised in **Supplementary Table S1** and **Table S2**, respectively.

The semi-circular and fully circular channels aimed to recreate a Strahler order 13 pulmonary artery (4) and were both 28 mm in length and radius of 2 mm. Both models contained the following 4 regions: pre-stenosis (8.5 mm length), stenosis (5 mm length), post-stenotic dilatation (2 mm length) and a downstream region (12.5 mm length) tapering to 1 mm and 2 mm diameter in the semi- and fully circular model, respectively, to model the natural tapering of a pulmonary artery. Concentric stenosis degrees of 30%, 60% and 80% were applied, and a straight channel (0% stenosis) was used as control. In both fully and semi-circular channels, the post-stenotic dilatation region had a width of 4 mm in the 30% and 60% stenosis models, while the same region had a width of 3 mm in the 80% stenosis model.

The moulds' dimensions were 36 mm x 20 mm x 7 mm (L x W x H). A 2 mm gap was left between the ends of the channels and the walls of the moulds.

**3D-printing of the semi-circular moulds.**

To create the PDMS devices, moulds with semi-circular channels were designed in Fusion 360 (AutoDesk) and printed in Model V2 resin (FormLabs), using a Form3 SLA 3D-printer (FormLabs). Resulting moulds were then washed for 2 x 5 min in isopropanol and cured for 30 min at 60°C. Supporting structures were manually removed.

The moulds were activated with silane prior to casting PDMS in order facilitate PDMS detachment after curing. Silanisation was performed in a cleanroom facility, by placing 20 µL of trichloro(chloromethyl)silane (Sigma-Aldrich, Cat no. 254436) on a glass slide in a vacuum desiccator alongside the moulds. Degassing was performed for 10 min, before turning the vacuum off and letting the moulds sit overnight.

PDMS was prepared by mixing 10 parts of elastomer to 1 part of curing agent (SYLGARD® 184, Dow Corning, Midland, MI, USA). The mixture was then slowly poured onto the moulds and left to cure for 24 h at 65°C.

The cured PDMS devices were peeled off the moulds and bonded to either glass coverslips (Ibidi, Cat no. 10812) for platelet adhesion assays, or polymer coverslips (ibiTreat coverslips, Ibidi, Cat no. 10812) for endothelial flow assays using PDMS, and set to cure at 65°C for 12 hours. Blunt needles (16G x 10 mm, tailored made from Coopers Needle Works, Ltd) were then inserted into the inlet and outlet regions bonded to the devices using PDMS. The edges of the bonded devices were sealed with another layer of PDMS to strengthen bonding to the coverslips, and the devices were left to cure again at 65°C for 12 hours. Completed models were flushed with absolute ethanol and left under UV light to sterilize for 4 hours.

**Characterization of the wall shear stress and flow patterns using computational fluid dynamics (CFD) analyses**.

All models were meshed in ICEM CFD (Ansys, Inc.). STL files created from Fusion 360 (Autodesk) were imported into the software. Surfaces were created from the imported, faceted geometries through the function "Create surface by angle", using an angle of 30 degrees. Inlet and outlet regions were created from the surfaces by using the function "create part – from surfaces". Curves for the inlet and outlet parts were created using the function "create curves – from surfaces". The main body of the geometry was defined as the "wall", where wall shear stress is applied in simulations. To define where the fluid should be perfused, another body was created inside the models by using the function "create body – as a centroid of 2 points".

Shell meshing parameters were set as an all-triangle mesh type, using a patch independent mesh method. The volume mesh type was set as tetra/mixed, using an Octree mesh method. Prisms were created at the wall and fluid parts. Part mesh element sizes were chosen depending on the overall mesh size to be achieved for the whole geometry.

After being computed, the mesh was repaired and smoothed as needed to achieve a mesh quality above 0.3. The final mesh was then exported to CFX-PRE (Ansys, Inc.) for pre-processing.

Meshes created in ICEM CFD (Ansys, Inc.) were imported into the pre-processing software CFX-PRE (Ansys, Inc.). All simulations were carried out in a laminar flow module and without thermal exchange. Water was used to simulate cell medium, using a dynamic viscosity of 1 mPa/s, a molar mass of 0.01802 kg/mol and a constant density of 992 kg/m$^3$. Blood was defined as a liquid with a density of 1060 kg/m$^3$,

a dynamic viscosity of 4 mPa/s and a molecular weight of 65 kg/mol. Inlet boundary conditions for water were adjusted to obtain similar hemodynamic conditions to those observed when simulations were run with blood. Outlet pressure was determined using a derivation of the Hagen-Poiseuille's equation (4), where $\mu$ is the dynamic viscosity, Q the inlet flow rate, $L_{tube}$ and $D_{tube}$ the length and inner diameter of the tubing used for flow perfusion, respectively.

$$P_{out} = \frac{128\mu Q L_{tube}}{\pi {D_{tube}}^4} \quad (4)$$

For semi-circular models, inlet velocities of 60.2 mm/sec (corresponding to a flow rate of 0.5 L/h) and 20 mm/sec (corresponding to a flow rate of 0.17 L/h) were used for water and blood, respectively. For fully circular models, inlet velocities of 50 mm/sec (corresponding to a flow rate of 2.26 L/h) and 15 mm/sec (corresponding to a flow rate of 0.68 L/h) were used for water and blood, respectively.
The inlet velocity values were chosen to achieve a WSS of 1 dyn/cm$^2$ in the straight, control channels, which corresponds to the average WSS seen in the large pulmonary arteries of healthy individuals.
Tubing inner diameter was set to 2.79 mm and 1.6 mm for the semi-circular models simulated with water and blood, respectively. A tubing inner diameter value of 2 mm was used for the fully circular models simulated with water and blood. Outlet pressures of 0.097 kPa and 1.16 kPa were used for the semi-circular models simulated with water and blood, respectively. For fully circular models, outlet pressures of 1.6 kPa and 1.92 kPa were used for water and blood, respectively. All inlet and outlet boundary parameters are summarised in **Table S3**.
A no-slip boundary condition was applied at the walls of the models. All simulations were run on the CFX Solver Manager (Ansys, Inc.).

**Post-processing.**
All results files were post-processed and analysed in CFD POST (Ansys, Inc.). Contours around the walls of the models were created to display wall shear stress (WSS) and pressure values. Velocity streamlines (50 data points), corresponding to the line tangential to the instantaneous velocity direction, were displayed from the inlet to show the flow patterns within the channels.
A polyline was created across the length of the channels to extract the exact WSS values. The polyline was derived from the intersection between the default domain (ie. the main body of the model) and YZ plane of the models. WSS, pressure and velocity values were then plotted against the Y axis of the models and extracted as a Microsoft Excel file for downstream analyses.
In the semi-circular channels, creating a polyline allowed the characterisation of WSS, pressure and velocity values at the top, curved wall of the models (referred to here as "top"), as well as the flat surface of the channel cross-section (named here as "bottom"). The average of the top and bottom values was therefore used when plotting final WSS, pressure, and velocity values against the Y axis of the model.

**Mesh Convergence Analyses.** A mesh sensitivity test was carried out to determine which mesh size to use for the final simulations. First, meshes of different sizes were created, aiming for a 2-fold increase in element size between each mesh. Quantitative comparison of mean WSS was performed at selected points in the channels: 7 mm (pre-stenosis), 11 mm (stenosis apex), 13.5 mm (post-stenotic dilatation apex), 18 mm (post-dilatation region 1) and 22.5 mm (post-dilatation region 2). WSS values from the top and bottom parts of the channels were averaged at each of these points and compared between each mesh. For all meshes, the % difference in WSS was determined between a selected mesh and a more refined mesh. A % difference of less than 5% was chosen as the cut-off to choose the final mesh, according to previous studies (430,431).

In the mesh sensitivity test, all simulations were performed with water, using an inlet velocity of 157 mm/sec (1.31 L/h) and an outlet pressure of 2.94 kPa. Part element sizes used for each mesh in the convergence analysis are provided in **Table S4**; Total number of elements for each mesh in **Table S5,** Mean WSS and % difference in WSS between meshes in each part of straight and stenotic channels in **Tables S6-S8**.

**Blood sample preparation.**
Venous blood was taken from antecubital veins of consenting, healthy donors. Samples were collected in 50 mL sterile falcon tubes and treated with 10% v/v acid citrate dextrose (ACD) (Sigma-Aldrich; Cat.no: C3821-50ML). Blood samples were used within 1 h of collection. 3,3-dihexyloxacarbocyanine iodide ($DiOC_6$) was added to the samples to stain for platelets.

**Platelet adhesion and aggregation assays in collagen-coated channels.**
Sterilised pulmonary artery models were coated with collagen type 1 (ChronoPAR, P/N 385; 120 µL/channel, 200 µg/mL) and left at room temperature for 2 hours. The channels were then blocked with 0.4% bovine serum albumin (in PBS, w//v). Citrated and $DiOC_6$-labelled blood was perfused through the coated channels using an Ibidi pump system for 4 minutes at a flow rate of 0.17 L/h (2.8 mL/min) or 0.50 L/h (8.3 mL/min). Fluorescent platelet aggregates were visualised with a fluorescent microscope (EVOS M5000, Invitrogen, Thermo Scientific). Platelet surface coverage was analysed with ImageJ (FIJI), using an in-house made macro developed by Stephen Rothery (Imperial College London, UK). All statistical analyses were performed on Prism 9 (GraphPad).

**Platelet adhesion and aggregation assays in endothelialised channels**.
Sterilised pulmonary artery models were coated with fibronectin (10 µl/mL in PBS; EMD Millipore Corp, USA, 341631), seeded with human pulmonary arterial endothelial cells (HPAECs; PromoCell, C-12241) and perfused with endothelial cell growth medium 2 (ECGM-2, PromoCell) for 6 hours or incubated overnight at 37°C under static conditions, to be used as static controls. The channels left under flow were disconnected from the flow system and perfused with citrated, $DiOC_6$-labelled whole blood at a flow rate of 0.17 L/h (2.8 mL/min) for 4 min each, using a syringe pump (Fisherbrand). The channels were then examined under a fluorescence microscope (Olympus IX70). Platelet surface coverage was analysed with ImageJ (FIJI).

**Cell culture.**
HPAECs (PromoCell, C-12241) were cultured in endothelial cell growth medium 2 (ECGM2; PromoCell, Germany C-22111) in fibronectin (10 µl/ml, EMD Millipore Corp, USA, 341631) coated 75cm2 tisue culture flasks (Sarstedt, C-22011). ECMG2 was supplemented with 2% Foetal Bovine Serum (FBS, Thermo Fisher Scientific, 10270098), Ascorbic Acid (1 µg/ml), Heparin (22.5 µg/ml), Hydrocortisone (0.2 µg/ml), 1% Penicillin-Streptomycin (100 µg/ml, Gibco, 15140-122), and the following growth factor mix (PromoCell, C-22111): Epidermal Growth Factor (EGF, 5 ng/ml), Basic Fibroblast Growth Factor (FGF, 10 ng/ml), Insulin-like Growth Factor (IGF, 20 ng/L), and Vascular Endothelial Growth Factor (VEGF, 0.5 ng/ml). HPAECs were used between passages 5-8.
Cells were cultured in a humidified incubator at 37 $^{o}$C under normoxic conditions (20% O2, 5% CO2) until 80% confluency. Media were changed every 2 days, and cells were passaged in a 1:3 split ratio. Briefly, cells were washed with phosphate-buffered saline (PBS; Sigma-Aldrich, USA, D8537), trypsinised with 0.05% Trypsin-EDTA (Thermo Fisher Scientific, USA, 25300062) for 4 minutes, before being resuspended in Dulbecco's Modified Eagle Medium (DMEM; Sigma-Aldrich, D6546) containing 10% FBS and 1% Streptomycin/Penicillin (100 µg/ml). Samples were then centrifuged at 1500 rpm for 5 minutes. Cell pellets were resuspended in ECGM2, and cells were counted prior to

seeding. Cells were used between passages 5-8. Cells displaying typical endothelial cell morphologies (cobblestone when confluent) were selected.
Cells to be used for future work were frozen by resuspending the pellet obtained after trypsinisation and centrifugation in 1 mL of 10% dimethysulfoxide (DMSO, Sigma-Aldrich) in FBS, transferred into cryotubes and stored in liquid nitrogen.
The arterial models were sterilised prior to cell seeding under ultraviolet light for 1h. Additionally, the channels were flushed with 70% ethanol and then 4 times with sterile PBS. After that, the channels were coated with fibronectin (10 µg/mL in PBS, EMD Milipore Corp, USA; 341631) for 1 h and washed with PBS. HPAECs, resuspended in ECGM-2 (7.0-8.0 x $10^5$ cells/mL), were introduced into the channels (100,000-120,000 cells/device) and incubated for 24 h to allow for complete cell adherence and monolayer formation. The cells were then either exposed to flow, left to incubate for longer if needed for experimental purposes, or fixed and stained for markers of interests.
To allow adaptation to flow, the cells were initially exposed to a low flow rate of 0.01 L/h (equivalent to a shear stress of 0.01 dyn/cm2 at the inlet) for 1h. The flow was then gradually increased by 0.1 L/h every hour, to reach the final flow rate of 0.5 L/h. After that, fresh medium was added to reservoirs and the cells were left under flow for 6 h or 24 h at 37°C. After the experiments, the devices were disconnected from the flow system and the tubing was flushed 1x with 0.2% sodium hydroxide (Sigma-Aldrich, cat no. S5881) in PBS (w/v), followed by 1x with distilled water. The tubing was autoclaved every 2 uses.

**Patient-derived Endothelial Colony Forming Cells**
Late outgrowth endothelial colony forming cells (ECFCs) were isolated from systemic blood from CTEPH patients (n=4) and 3 control healthy individuals. Donor characteristics are summarized in **Table S9**.
Briefly, ECFCs CTEPH patients were isolated by diluting freshly donated blood with PBS in a 1:1 ratio and transferring the mixture into falcon tubes filled with 15 mL of LymphoprepTM (Stemcell technologies; Cat: 07851). Samples were then centrifuged for 30 min at 0.5 RCF at 20°C, and the interface of Ficoll gradients and a part of the enriched plasma were transferred into a fresh falcon tube. 40 mL of PBS was then added to the falcon tube and the mixture was centrifuged for 5 min at 0.3 RCF at RT, decanted and the pellet was resuspended with 20 mL of PBS. The cell suspension was then centrifuged for 10 min at 0.2 RCF at RT, resuspended in 15 mL of cell medium and the final mixture was plated into each well of a 6-well collagen-coated plate (2-3 mL per well). Medium was changed on the following day, and then every 2 days until cell colonies appeared (around 3 weeks post-seeding).
ECFCs were initially cultured in ECGM-2 medium (ECGM2; PromoCell, Germany C-2211, supplemented with 20% HyClone Characterized Fetal Bovine Serum (Cytiva; Cat:SH30071.03IH25-40), Ascorbic Acid (1 µg/mL), Heparin (22.5 µg/mL), Hydrocortisone (0.2 µg/mL), 1% Penicillin-Streptomycin (100 µg/mL, Gibco, 15140-122), 1% L-Glutamine (Gibco™, 200mM, A2916801) and the growth factor supplement (PromoCell, C-22111) containing Epidermal Growth Factor (EGF, 5 ng/mL), Basic Fibroblast Growth Factor (FGF, 10 ng/mL), Insulin-like Growth Factor (IGF, 20 ng/L), and Vascular Endothelial Growth Factor (VEGF, 0.5 ng/mL)) until colonies appeared. After that, ECGM-2 supplemented with the growth factor mix, 10% HyClone FBS and antibiotics was used for passaging cells.
Cells were then grown until full confluency, trypsinised, pelleted and transferred into a gelatin-coated 75cm2 tissue culture flask.

**Culture of pulmonary endarterectomy endothelial cells**
PEA cells from 2 CTEPH patients were extracted from fresh PEA lung tissue samples, taken from the right inferior lobe and left superior lobe, respectively. Briefly, the tissues were first cut into small pieces and added to the wells of a 6-well plate coated with 0.2% gelatin (Sigma; Cat: G1890). 2 mL of ECGM-

2 medium (PromoCell, Germany; Cat: C-2211) supplemented with 10% HyClone FBS (Cytiva; Cat:SH30071.03IH25-40) and 1% Penicillin-Streptomycin (100 µg/mL, Gibco, 15140-122) was added to each well. The following day, 1mL of medium was replaced with fresh medium, and the procedure repeated for the next 3 days. The medium was then fully replaced with fresh medium every 2 days, without removing the pieces of tissue, for the next 6 days. After this, medium was changed, and the pieces of tissue slowly removed over a week. Full ECGM-2 supplemented with 10% HyClone FBS and 1% Penicillin-Streptomycin was used until colony formation.
PEA cells were then passaged and cultured in 0.2% gelatin (Sigma; Cat: G1890)-coated 75cm2 tissue culture flasks (Sarstedt; Cat: C-22011), in full ECGM-2 medium (ECGM2 (PromoCell, Germany; Cat: C-2211), supplemented with 2% Foetal Bovine Serum (FBS, Thermo Fisher Scientific, 10270098), Ascorbic Acid (1 µg/mL), Heparin (22.5 µg/mL), Hydrocortisone (0.2 µg/mL), 1% Penicillin-Streptomycin (100 µg/mL, Gibco, 15140-122) and the following growth factor mix (PromoCell; Cat: C-22111): Epidermal Growth Factor (EGF, 5 ng/mL), Basic Fibroblast Growth Factor (FGF, 10 ng/mL), Insulin-like Growth Factor (IGF, 20 ng/L), and Vascular Endothelial Growth Factor (VEGF, 0.5 ng/mL)).
PEA cells were cultured in a humidified incubator supplemented with 5% CO2 at 37°C until 80% confluency. Media were changed every 2 days, and cells were passaged in a 1:3 split ratio, as previously described. Endothelial identity of the PEA cells was confirmed according to previously described methods (193). Patient characteristics are summarized in Table S9.

**Flow system.**
The channels were perfused using a closed-circuit system driven by a REGLO ICC 4 channel 12 Roller Pump (Cole-Parmer, UK, cat no. ISM4412). The pump was connected to two medium reservoirs acting as capacitators (ref), placed before and after the inlet and outlet of the PDMS device, respectively. The reservoirs had a total capacity of 2 mL, with two hose barb connectors to connect the tubing to both the pump and the device's inlet or outlet. The tops of the reservoirs have a screw thread to fit commercially available microcentrifuge tube caps lined with a silicone O-ring (Greiner Bio-One, 12 mm screw cap; Cat no.: 366380). Two small extensions were added to the bottom of the reservoir to secure them to a baseplate.
The peristaltic pump was connected to each reservoir using Ismatec® Pump Tubing, 3-stop, PharMed® BPT tubing, 2.76 mm ID (Cole-Parmer, UK, cat no. WZ-95714-48) and Ismatec® Pump Tubing, PharMed® BPT extension tubing, 2.76mm ID; 100ft (Cole-Parmer, UK, cat no. WZ-95809-48). Short pieces of Ismatec® Pump Tubing, PharMed® BPT extension tubing, 1.14 mm ID; 100ft (Cole-Parmer, UK, cat no. WZ-95809-30) were used to connect the end of the 2.79 mm ID tubing to the barbs of each reservoir. The same 1.14 mm ID tubing was used to connect the inlet and outlet of the devices to the lower barbs of the reservoir.
The size of the tubing (2.79 mm ID) was chosen based on the flow rate needed to be achieved. The smaller 1.14 mm ID tubing connecting the devices with media reservoirs was used to create additional resistance and further dampen the oscillations generated by the pump. This set-up was optimized after carrying out flow rate measurements.

**Flow rate measurements**.
Fow rate measurements were performed using a Sensirion SLF3S-1300F flow sensor (Mouser electronics, cat no. 403-SLF3S-1300F). The flow circuit was primed with distilled water (as per the manufacturer's instructions) prior to testing, by connecting the inlet and outlet tubing together using a blunt needle and filling in the outlet reservoir until the inlet reservoir became full. After priming, the devices were connected to the reservoirs via tubing and perfused with distilled water for 1 min at a flow rate of 0.5 L/h (8.63 mL/min). The flow sensor was then placed between the outlet of the channel and the reservoir, and connected via USB cable to a laptop, on which waveforms measurements were

performed using the Sensirion Control Center software (Sensirion). Data was acquired for 1 min at a flow rate of 0.5 L/h and analyzed using the Sensirion Data Viewer software (Sensirion).

The shear rate in the selected regions of the channel can be determined using the formula below:

$$SR = \frac{WSS}{\eta} \quad (4)$$

Where SR is the shear rate ($s^{-1}$), WSS the wall shear stress (Pa) and η the dynamic viscosity ($Pa.s^{-1}$).

**Viability assay.**
The LIVE/DEAD™ Viability/Cytotoxicity kit (ThermoFisher, cat no. L3224) was used to perform cell survival analyses. The cells were imaged under an inverted fluorescent microscope (Olympus IX70).

**Immunostaining and cell imaging.**
HPAECs were fixed with 4% paraformaldehyde (PFA; Sigma Aldrich, UK) (w/v) in PBS for 20 min and permeabilised with 0.5% Triton X-100 (Sigma Aldrich, UK) (v/v) in PBS for 5 min. The cells were washed three times with PBS between each step. HPAECs were then blocked in 2% BSA (A9418, Sigma Aldrich, UK) (w/v) in PBS for 30 min and incubated with Alexa Fluor 488-conjugated mouse monoclonal anti-VE-Cadherin antibody (eBioscience, cat no. 53-1449-42, 1:100) and TRITC-Phalloidin in 1% BSA (w/v) in PBS for 2 h at room temperature in the dark. The channels were washed three times with PBS, mounted with DAPI in VectashieldÒ (Vector Laboratories) and imaged under an inverted fluorescent microscope (Olympus IX70) or a confocal microscope (Leica Stellaris 8).
Cell coverage and cell alignment analyses were carried out in ImageJ (FIJI). Cells were considered aligned to flow if the angle between nuclear long axis and flow direction was below 30°.

**Flow exposure of patient-derived Endothelial Colony Forming Cells**
ECFCs cultured in 60% stenosis channels were exposed to flow. This level of stenosis was selected as it was the smallest degree of stenosis found to significantly affect endothelial structure and function.
Briefly, the channels were coated with 0.2% gelatin (Sigma; Cat: G1890) and left to incubate for at least 10min at 37oC. The gelatin was then removed, and the channels were left to air-dry. ECFCs were resuspended in ECFCs-specific ECGM-2 (7.0-8.0x105 cells/mL) and introduced into the channels (100,000-120,000 cells/device). The cells were incubated for 24h to allow for complete cell adherence and monolayer formation. The cells were then either exposed to flow for 6h or were fixed and stained for markers of interests.

**RNA extraction, Reverse Transcription and qPCR**
Prior to RNA extraction, surfaces, pipettes, and tip boxes were sprayed with RNaseZAP (Invitrogen; Cat no: AM9780). To isolate cells from different parts of the microfluidic channels, regions of interest (ROIs) termed “upstream”, “stenosis”, “post-stenotic dilatation”, and “downstream” were marked with a pen at the bottom side of the thin polymer coverslips. Culture medium was removed and the PDMS chamber was peeled off the coverslips.
ROIs with cells still attached were carefully cut out with sterile scissors and transferred directly into DNA/RNA-free tubes filled with 500 µL TRIzolTM Reagent (Thermo Scientific; Cat: 15596026 ) and incubated for 5 min at RT. After 2-3 gentle shakes to dislodge cells, plastic cutouts were removed from the tubes with sterile tweezers and the remaining cell suspension was vortexed for 1 min and placed on ice or stored at –80o C for future use. Samples were kept on ice until all ROIs were collected.
To extract RNA, samples were incubated for 5 min at RT. 140 µL of RNase-free Chloroform was then added to the samples and pipetted up and down thoroughly 10 times. The samples were inverted to mix for 20 seconds, incubated at RT for 2-3min and centrifuged at 12,000 g for 15 min at 4oC.

The upper aqueous phase (300 µL) was transferred to new RNase-free tubes and 4 µL glycogen (5 mg/mL; Thermo Scientific; Cat: AM9510) was added to the samples, followed by 450 µL of RNase, DNase, and Protease-free 99.5% isopropanol (Thermo Scientific; Cat: 327272500). Tubes were gently inverted to mix for 10 seconds and incubated at 4 oC for 10 min.
Samples were then centrifuged at 12,000 g for 10 min at 4 oC, the supernatant was removed, and resulting pellets were resuspended in 75% Ethanol (Fisher Scientific) in UltraPure™ DNase/RNase-Free Distilled Water (Invitrogen; Cat:11538646) and vortexed gently. The samples were centrifuged again or 5 min at 7,500 g at 4 °C, the supernatant was removed, and the pellets were left to dry on ice for 8-10 min. The samples were finally resuspended in 20 µL UltraPure™ DNase/RNase-Free Distilled Water (Invitrogen; Cat: 11538646) and the RNA concentration was measured on a NanoDrop™ ND2000 spectrophotometer (Thermo Scientific). RNA purity was assessed by the ratio of absorbance at 260 nm and 280 nm (A260/A280). Values above 1.8 were considered of acceptable quality. RNA samples were stored at –80oC for future experiments.

**Tables S10-S14** provide details of qPCR reverse transcription mix, RT cycling conditions, list of primers, components of qPCR reactions and amplification and cycling conditions.

50-200 ng of RNA (extracted as described in 5.1.4) were reverse transcribed into cDNA using a LunaScript Reverse Transcription (RT) SuperMix Kit (New England Biolabs, MA, USA; Cat: E3010L).

The samples were prepared on ice into 200 µL RNase-free tubes according to details in Table 5.2 to a final volume of 20 µL. Samples were then flicked and spinned down, before being reverse transcribed into cDNA using a SimpliAmpTM Thermal Cycler (Applied Biosystems, UK).
The No-RT Control Mix (5x) was used to make negative controls to check for DNA contamination. cDNA samples were then all diluted with 30-180 µL RNase free water (depending on the starting amount of RNA used) to a make a final 1 ng/µL cDNA solution. cDNA samples were either stored at –20°C or directly used for qPCR.

All primer sequences were designed from FASTA sequences (PubMed, NCBI). Briefly, coding sequences (CDS) were copy-pasted into the Primer3web website (https://primer3.ut.ee) and primer picking conditions were set as outlined in Figure 5.1. Primer pairs of identical lengths were preferably selected, and their sequences input into Primer-BLAST (NCBI) to check for their gene specificity. Primer pairs were retained only if they specifically matched the gene of interest.
Selected primers (DNA oligos) were ordered from Sigma-Aldrich, reconstituted with RNase-free water according to the manufacturers' instructions and stored at –20 °C.

All samples were prepared on ice. 9 µL of Luna® Universal qPCR Master Mix (New England Biolabs, MA, USA; Cat: M3003X) and 1 µL of 1 ng/µL cDNA (prepared as described in 6.1.5) were added to each well of a 384-well PCR plate (Thermo Fisher Scientific; Cat: AB1384). A negative control for each gene of interest, consisting of 1µL Nuclease-free water instead of 1 µL cDNA, plus 9 µL of appropriate qPCR master mix, was added to the plate. Details of the components used in the reactions are outlined in Table 5.5.
Plates were sealed with clear adhesive PCR plate seals (Thermo Fisher Scientific; Cat: AB0558) and centrifuged for 1 minute at 1100 g. qPCR was performed using a QuantStudio 12K Flex Real-Time PCR System (Applied Biosystems, USA). Details of the qPCR amplification cycles are provided in Table 5.6.
All qPCR amplifications were performed with a QuantStudio 12K Flex Real-Time PCR System (Applied Biosystems, USA).
The relative gene expression was determined using the 2-ΔCt method (480) with target genes normalised to Beta-2-Microglobulin (B2M) expression. This method was chosen to present the data as normalised, individual data points. All data analyses were carried out in PRISM 9 (GraphPad 2023).

A p-value of less than 0.05 was considered statistically significant. Unpaired t-tests were used to compare gene expression between 2 different

**SUPPLEMENTAL FIGURES**

Salina Nicoleau et al. 3D Modelling of Pulmonary Arterial Geometry and Endothelial Dysfunction in CTEPH

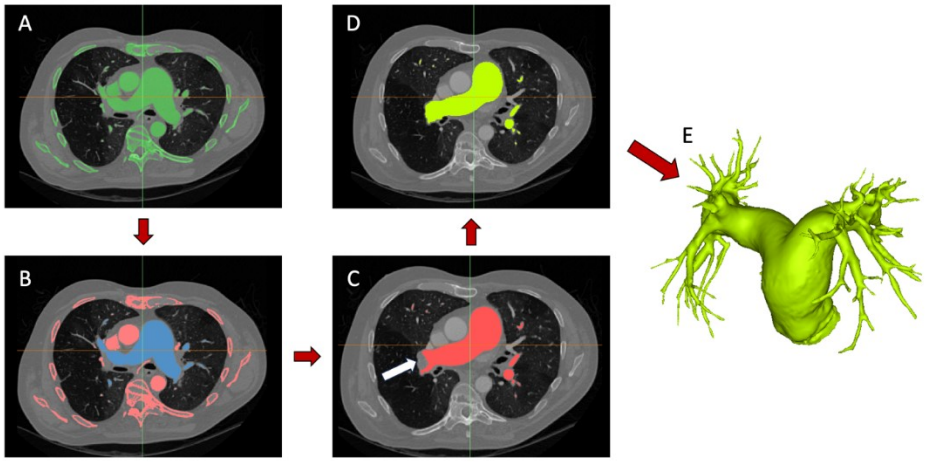


**Figure S1. CTPA segmentation process with the Mimics software**

Outline of the CTPA segmentation process on Mimics 23.0 (Materialise, 2021). First, a mask is created to separate cardiovascular components from bones and fat tissues by adjusting the Hounsfield Units threshold (A). The mask is then split into two to differentiate the pulmonary arteries (blue) from other components (red) (B). When an occluding thrombus is present (C, white block arrow), the mask is manually filled by following the outer lining of the arteries (D). A 3D model is then reconstructed, and its surfaces smoothed out (E).

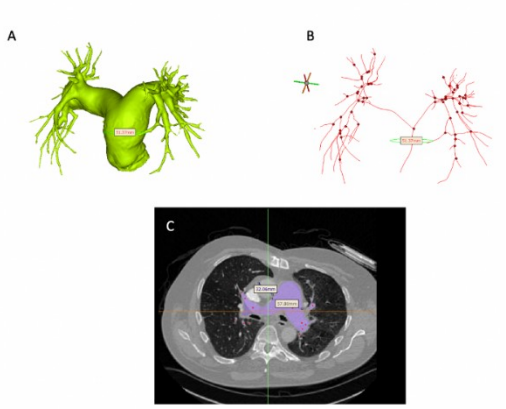


**Figure S2. Best fit diameters and rPA measurements**

Best fit diameters of the main pulmonary artery shown in the 3D-reconstructed model (A) and centerline (B). Pulmonary artery-to-ascending aorta ratio (rPA) measurement on the axial view (C). All measurements were made on Mimics 23.0 (Materialise, 2021). A total of 16 CTPAs were segmented and analysed, of which 7 were from CTEPH, four from APE, two from CTED and three from non-PE patients. Non-PE patients (n=3) were used as controls

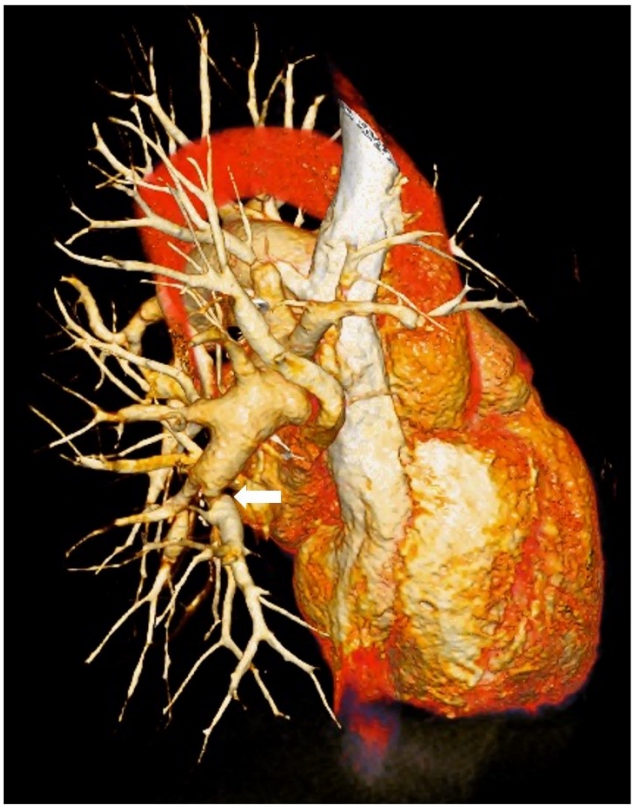

**Figure S3. Examples of "ring"-like stenoses in CTEPH patients**
"Ring"-like stenoses observed in patients with chronic thromboembolic pulmonary hypertension (CTEPH). (A) shows the axial view of a computed tomography pulmonary angiogram in a patient with proximal CTEPH. The thin arrow points to a proximal web and stenosis in the left upper lobe pulmonary artery, with a post stenotic dilatation (block arrow with red outline). A complete occlusion of the right upper lobe artery can also be seen (notched arrow). (B). CT Volume Rendered image demonstrates a tight stenosis followed by post stenotic dilatation (block arrow) in the right lower lobe pulmonary artery. Images obtained with the courtesy of Dr Deepa Gopalan (Imperial College Healthcare NHS Trust, London, UK).

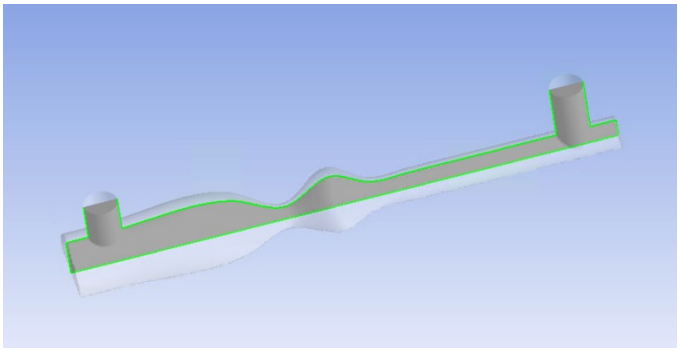

**Figure S4. Polyline for the 60% stenosis semi-circular model**
The polyline was created by taking the intersection between the default domain (ie the vascular model) and YZ plane of the model. The polyline was then used to extract wall shear stress, pressure, and velocity values for downstream analyses.

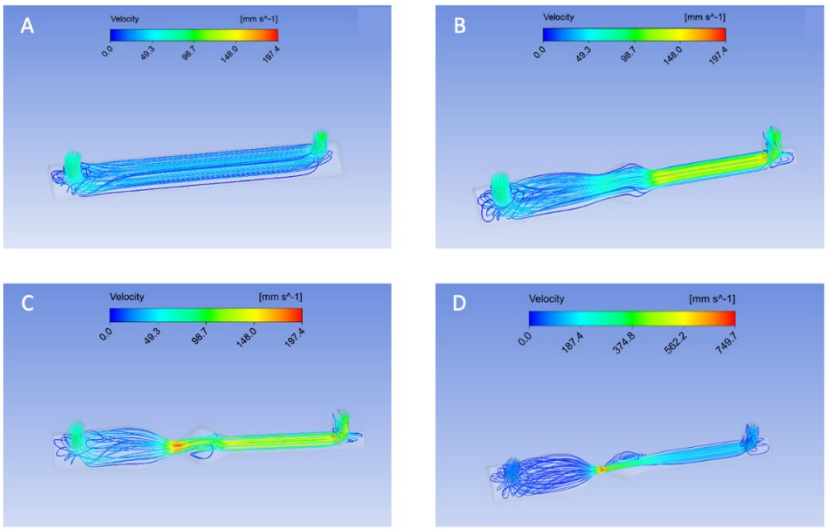


**Figure S5. Velocity streamlines in semi-circular channels (simulated with water)**
Computational fluid dynamics (CFD) results showing velocity streamlines in the control (A), 30% stenosis (B), 60% stenosis (C) and 80% stenosis (D) models. Simulations were run with water, using an inlet velocity of 60.2 mm/sec (corresponding to a flow rate of 0.5L/h) and an outlet pressure of 0.097 kPa. Colour scales at the top of the images in (A)-(C) represent a velocity range between 0.0-197.4 mm/s, while in (D) the sale ranges from 0.0-749.7 mm/s. All simulations were performed in CFX (Ansys, Inc.).

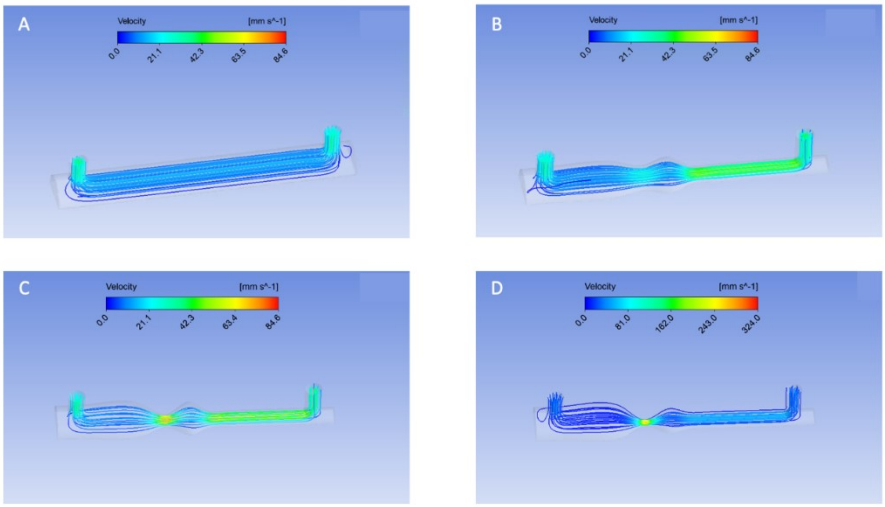


**Figure S6. Velocity streamlines in semi-circular channels (simulated with blood)**
Computational fluid dynamics (CFD) results showing velocity streamlines in the control (A), 30% stenosis (B), 60% stenosis (C) and 80% stenosis (D) models. Simulations were run with blood, using an inlet velocity of 20 mm/sec (corresponding to a flow rate of 0.17 L/h) and an outlet pressure of 1.16 kPa. Colour scales at the top of the images in (A-C) represent a velocity range between 0.0-84.6 mm/sec, while in (D) the scale ranges from 0.0-324.0 mm/sec. All simulations were performed in CFX (Ansys, Inc.).

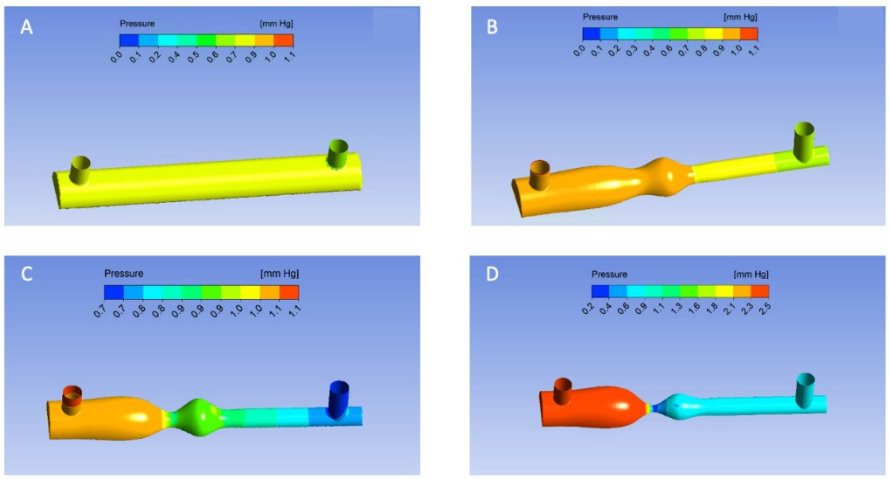


**Figure S9. Pressure changes in semi-circular channels (simulated with water)**
Computational fluid dynamics (CFD) results showing pressure values within the control (A), 30% stenosis (B), 60% stenosis (C) and 80% stenosis (D) channels. Simulations were run with water, using an inlet velocity of 60.2 mm/sec (corresponding to a flow rate of 0.5 L/h) and an outlet pressure of 0.097 kPa. Colour scales at the top of the images in (A-C) represent a pressure range between 0.0-1.1 mmHg, while in (D) the scale ranges from 0.0-2.5 mmHg. All simulations were performed in CFX (Ansys, Inc.).

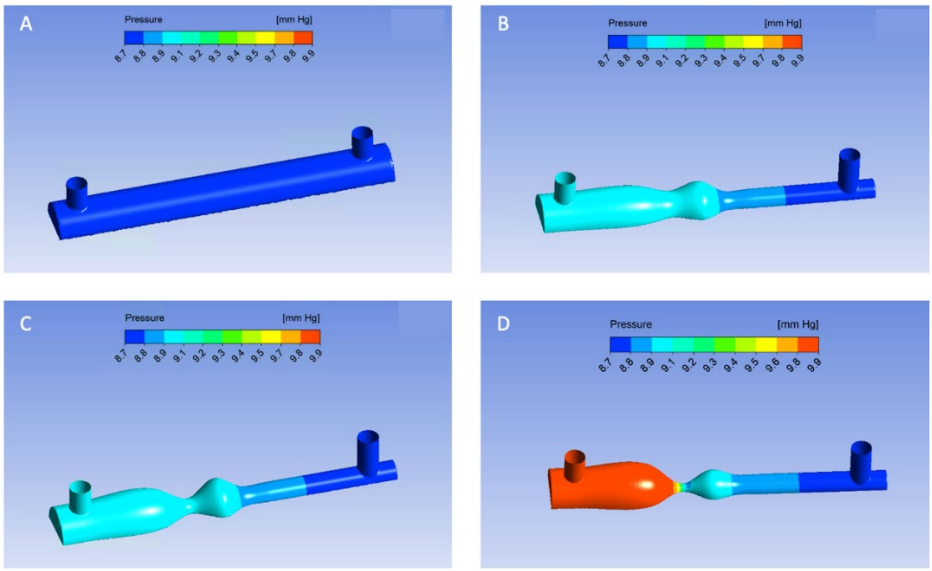


**Figure S10. Pressure changes in semi-circular channels (simulated with blood)**
Computational fluid dynamics (CFD) results showing pressure values within the control (A), 30% stenosis (B), 60% stenosis (C) and 80% stenosis (D) channels. Simulations were run with blood, using an inlet velocity of 20 mm/sec (corresponding to a flow rate of 0.17 L/h) and an outlet pressure of 1.16 kPa. Colour scales at the top of the images represent a pressure range between 0.0-9.9 mmHg. All simulations were performed in CFX (Ansys, Inc.).

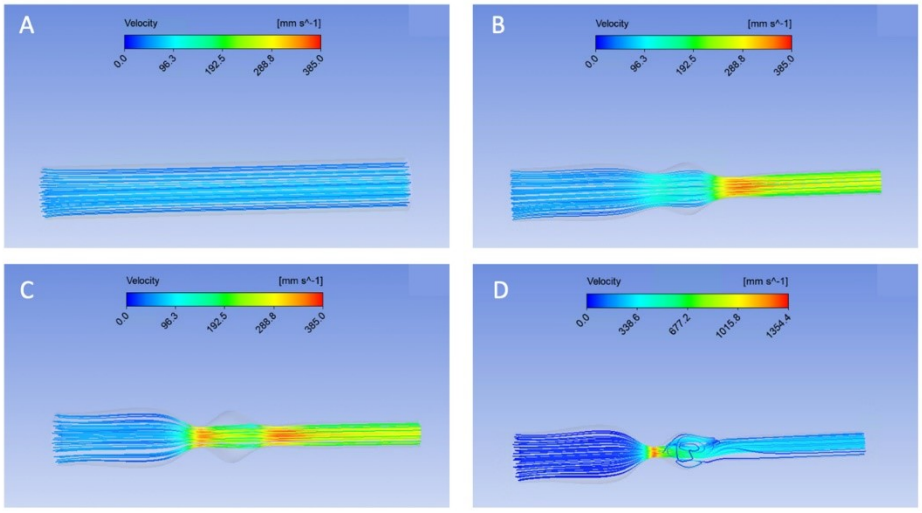


**Figure S11**. **Velocity streamlines in fully circular channels (simulated with water)**
Computational fluid dynamics (CFD) results showing velocity streamlines in the fully circular control (A), 30% stenosis (B), 60% stenosis (C) and 80% stenosis (D) models. Simulations were run with water, using an inlet velocity of 50 mm/sec (corresponding to a flow rate of 2.26 L/h) and an outlet pressure of 1.60 kPa. Colour scales at the top of the images in (A)-(C) represent a velocity range between 0.0-385 mm/sec, while in (D) the scale ranges from 0.0-1354.4 mm/sec. All simulations were performed in CFX (Ansys, Inc.).

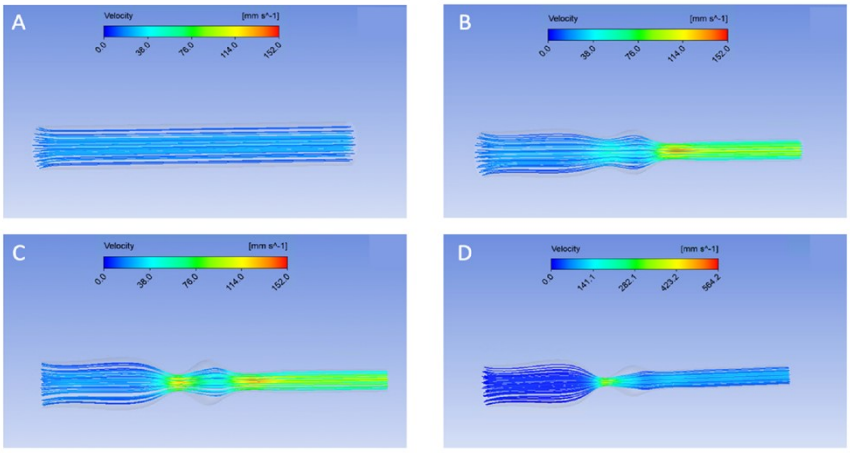


**Figure S12**. **Velocity streamlines in fully circular channels (simulated with blood)**
Computational fluid dynamics (CFD) results showing velocity streamlines in the fully circular control (A), 30% stenosis (B), 60% stenosis (C) and 80% stenosis (D) models. Simulations were run with blood, using an inlet velocity of 15 mm/sec (corresponding to a flow rate of 0.68 L/h) and an outlet pressure of 1.92 kPa. Colour scales at the top of the images in (A)-(C) represent a velocity range between 0.0152.0 mm/sec, while in (D) the scale ranges from 0.0-564.2 mm/sec. All simulations were performed in CFX (Ansys, Inc.).

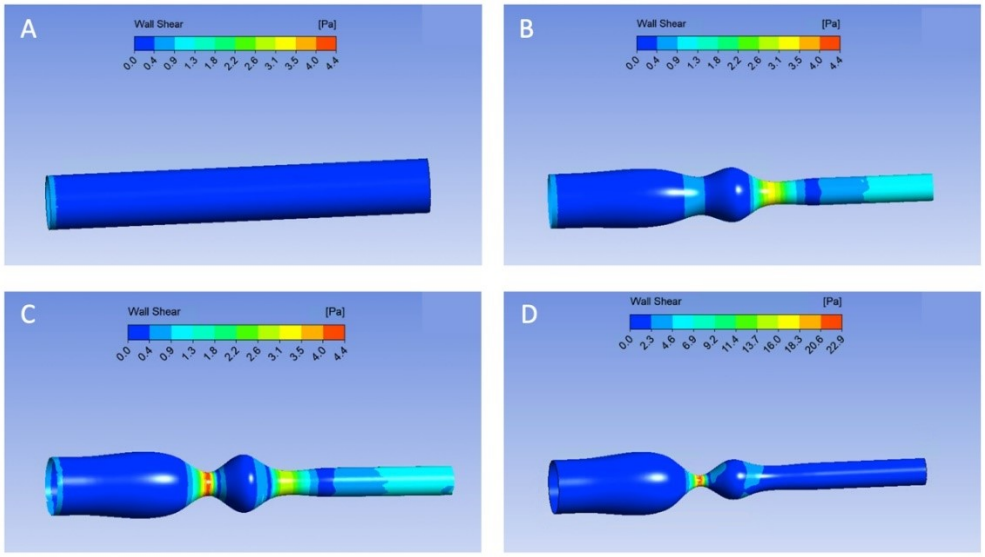


**Figure S13. Wall shear stress in fully circular channels (simulated with water)**
Wall shear stress (WSS) in the fully circular control (A), 30% stenosis (B), 60% stenosis (C) and 80% stenosis (D) models. Simulations were run with water, using an inlet velocity of 50 mm/sec (corresponding to a flow rate of 2.26 L/h) and an outlet pressure of 1.60 kPa. Colour scales at the top of the images in (A)-(C) represent a WSS range between 0.0-4.4 Pa (0.0-44 dyn/cm$^2$), while in (D) the scale ranges from 0.0-22.9 Pa (0.0-229 dyn/cm$^2$). All simulations were performed in CFX (Ansys, Inc.). 1 Pa = 10 dyn/cm$^2$.

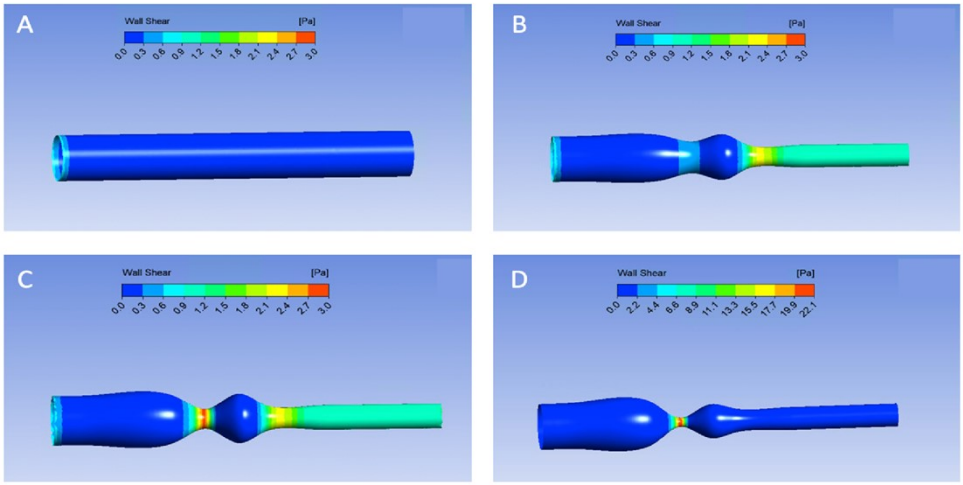


**Figure S14**. **Wall shear stress in fully circular channels (simulated with blood)**
Wall shear stress (WSS) in the fully circular control (A), 30% stenosis (B), 60% stenosis (C) and 80% stenosis (D) models. Simulations were run with blood, using an inlet velocity of 15 mm/sec (corresponding to a flow rate of 0.68 L/h) and an outlet pressure of 1.92 kPa. Colour scales at the top of the images in (A)-(C) represent a WSS range between 0.0-3.0 Pa (0.0-30.0 dyn/cm$^2$), while in (D) the scale ranges from 0.0-22.1 Pa . All simulations were performed in CFX (Ansys, Inc.).

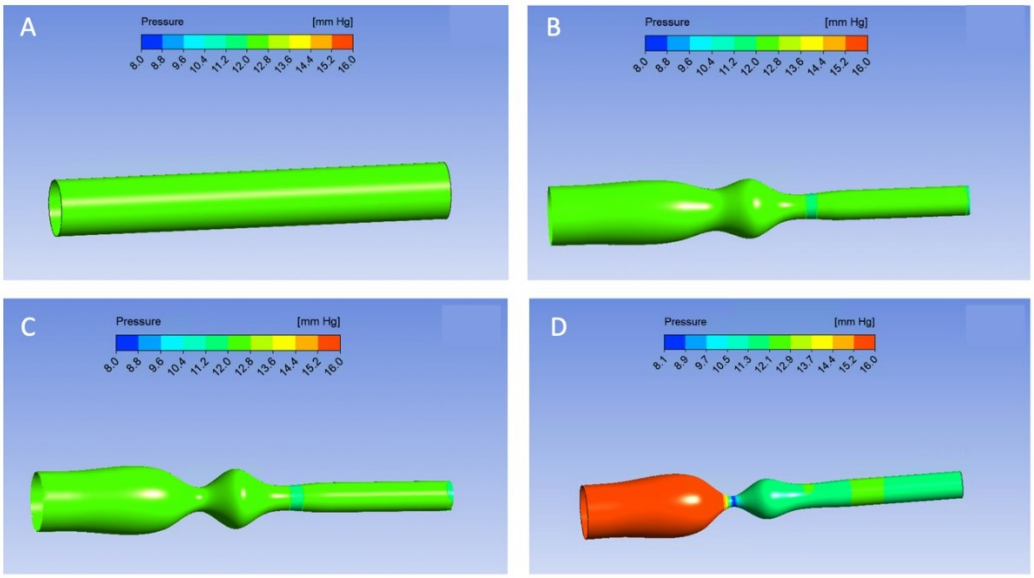


**Figure S15**. **Pressure changes in fully circular channels (simulated with water)**
Computational fluid dynamics (CFD) results showing pressure in the fully circular control (A), 30% stenosis (B), 60% stenosis (C) and 80% stenosis (D) models. Simulations were run with water, using an inlet velocity of 50 mm/sec (corresponding to a flow rate of 2.26 L/h) and an outlet pressure of 1.60 kPa. Colour scales at the top of the images represent a pressure range between 0.0-16.0 mmHg. All simulations were performed in CFX (Ansys, Inc.).

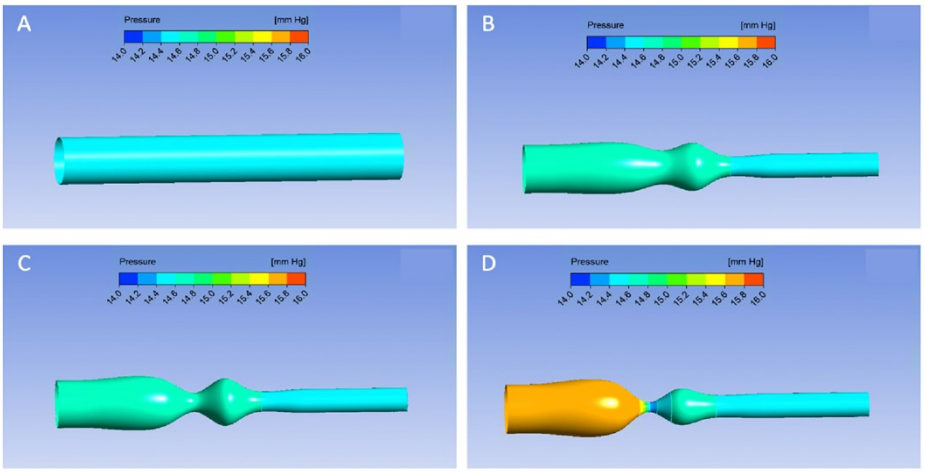


**Figure S16**. **Pressure changes in fully circular channels (simulated with blood)**
Computational fluid dynamics (CFD) results showing pressure in the fully circular control (A), 30% stenosis (B), 60% stenosis (C) and 80% stenosis (D) models. Simulations were run with blood, using an inlet velocity of 15 mm/sec (corresponding to a flow rate of 0.68 L/h) and an outlet pressure of 1.92 kPa. Colour scales at the top of the images represent a pressure range between 0.0-16.0 mmHg All simulations were performed in CFX (Ansys, Inc.).

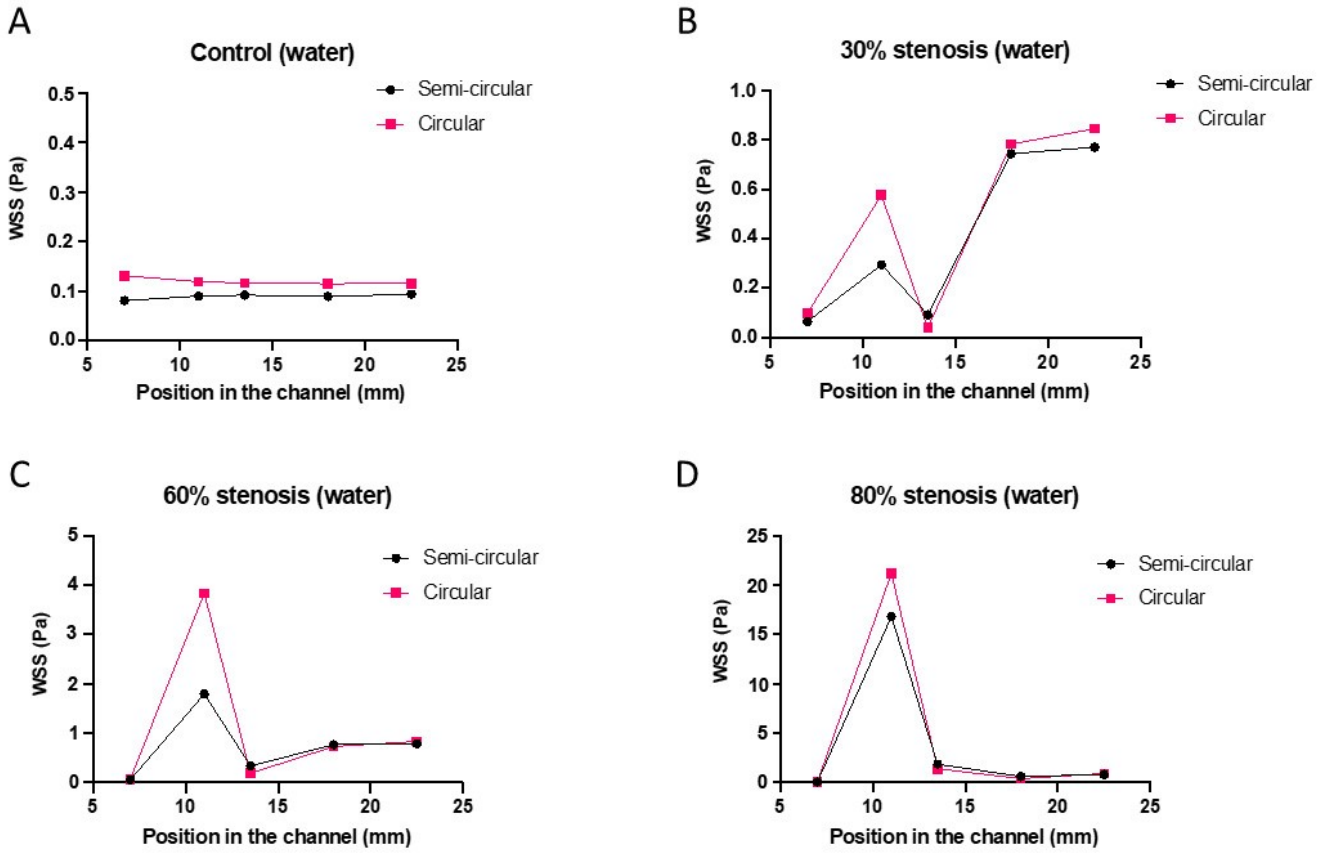


**Figure S17. Wall shear stress in semi-circular and fully circular models for simulations run with water.** Comparison of wall shear stress (WSS) values in the semi-circular and fully circular control (A), 30% (B), 60% (C) and 80% (D) stenosis models for simulations run with water. The X axis indicates the different regions of the channel: upstream/pre-stenosis (7 mm), stenosis (11 mm), post-stenotic dilatation (13.5 mm), downstream (18 mm and 22.5 mm). Simulations were performed in CFX (Ansys, Inc.), using an inlet velocity of 60.2 mm/sec (0.5 L/h) and outlet pressure of 0.097 kPa for the semi-circular channels, and an inlet velocity of 50 mm/sec (2.26 L/h) and outlet pressure of 1.60 kPa for the fully circular channels.

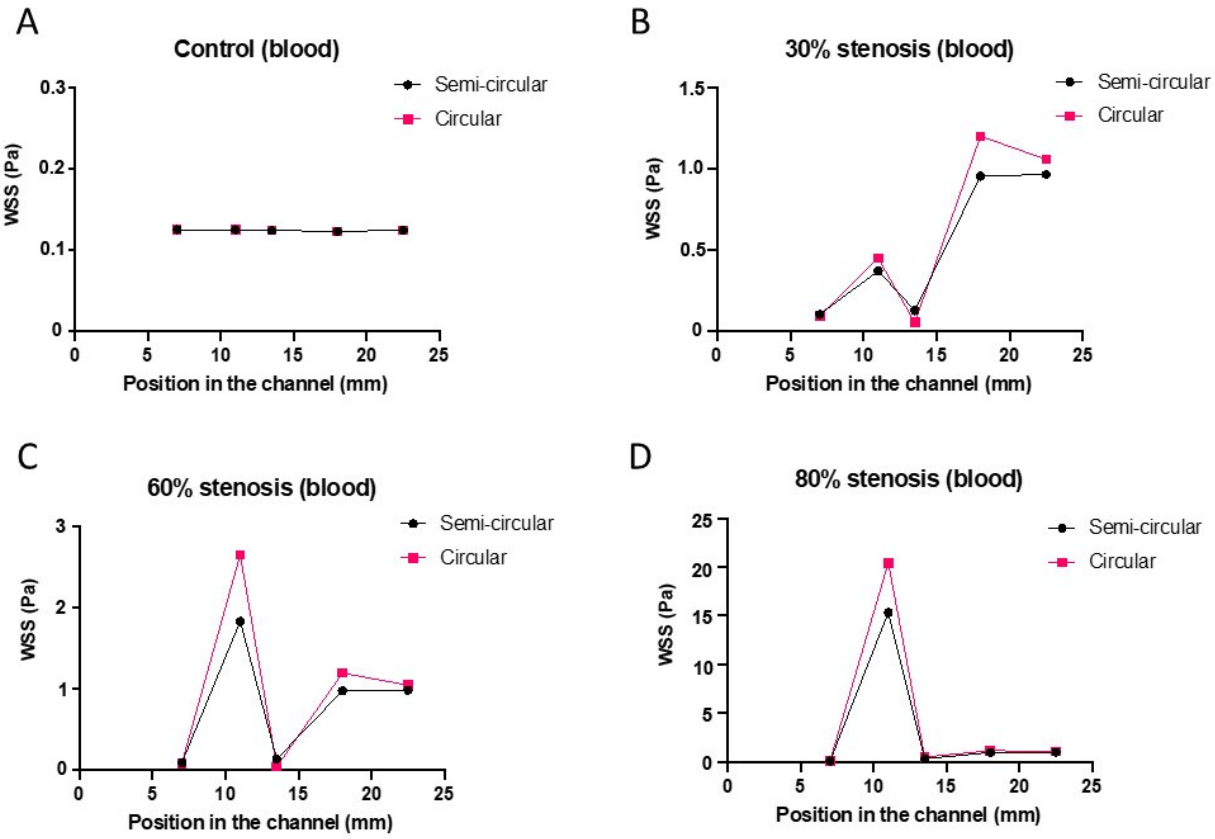


**Figure S18. Wall shear stress in semi-circular and fully circular models for simulations run with blood.** Comparison of wall shear stress (WSS) values in the semi-circular and fully circular control (A), 30% (B), 60% (C) and 80% (D) stenosis models for simulations run with blood. The X axis indicates the different regions of the channel: upstream/pre-stenosis (7 mm), stenosis (11 mm), post-stenotic dilatation (13.5 mm), downstream (18 mm and 22.5 mm). Simulations were performed in CFX (Ansys, Inc.), using an inlet velocity of 20mm/sec (0.17 L/h) with an outlet pressure of 1.16 kPa for the semi-circular channels, and an 15 mm/sec (0.68 L/h) with an outlet pressure of 1.92 kPa for the fully circular channels.

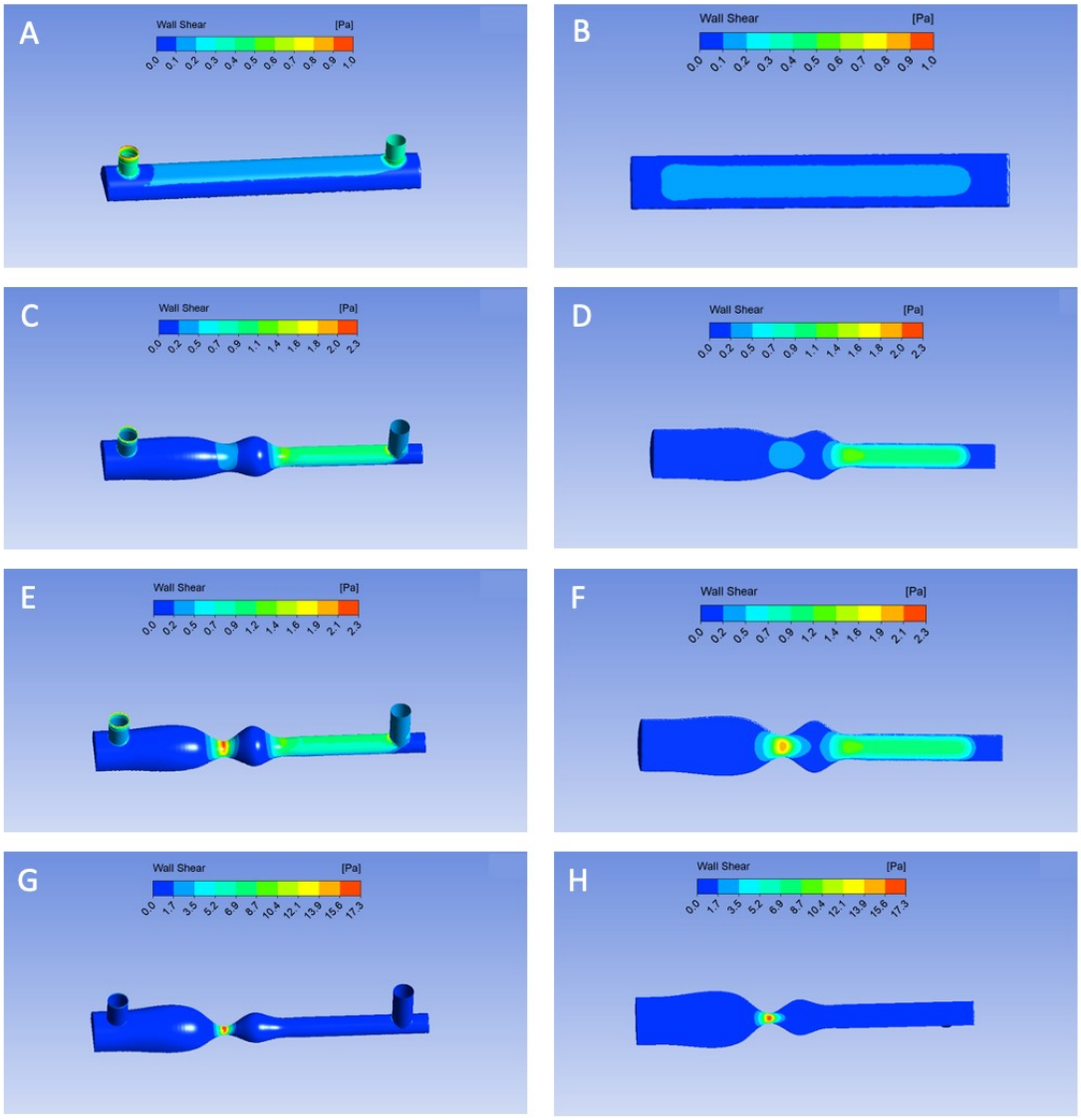


**Figure S19. Wall shear stress in semi-circular channels (simulated with blood)**
Computational fluid dynamics (CFD) results showing wall shear stress (WSS) at the top and bottom of the semi-circular channels in the control (A), 30% stenosis (B), 60% stenosis (C) and 80% stenosis (D) models. Simulations were run with blood, using an inlet velocity of 20 mm/sec (corresponding to a flow rate of 0.17 L/h) and an outlet pressure of 1.16 kPa. Colour scales at the top of the images in (A)-(F) represent a WSS range between 0.0-2.3 Pa (0.0-23 dyn/cm$^2$), while in (G-H) the scale ranges from 0.0-17.3 Pa (0.0-173 dyn/cm$^2$). All simulations were performed in CFX (Ansys, Inc.). 1 Pa = 10 dyn/cm$^2$.

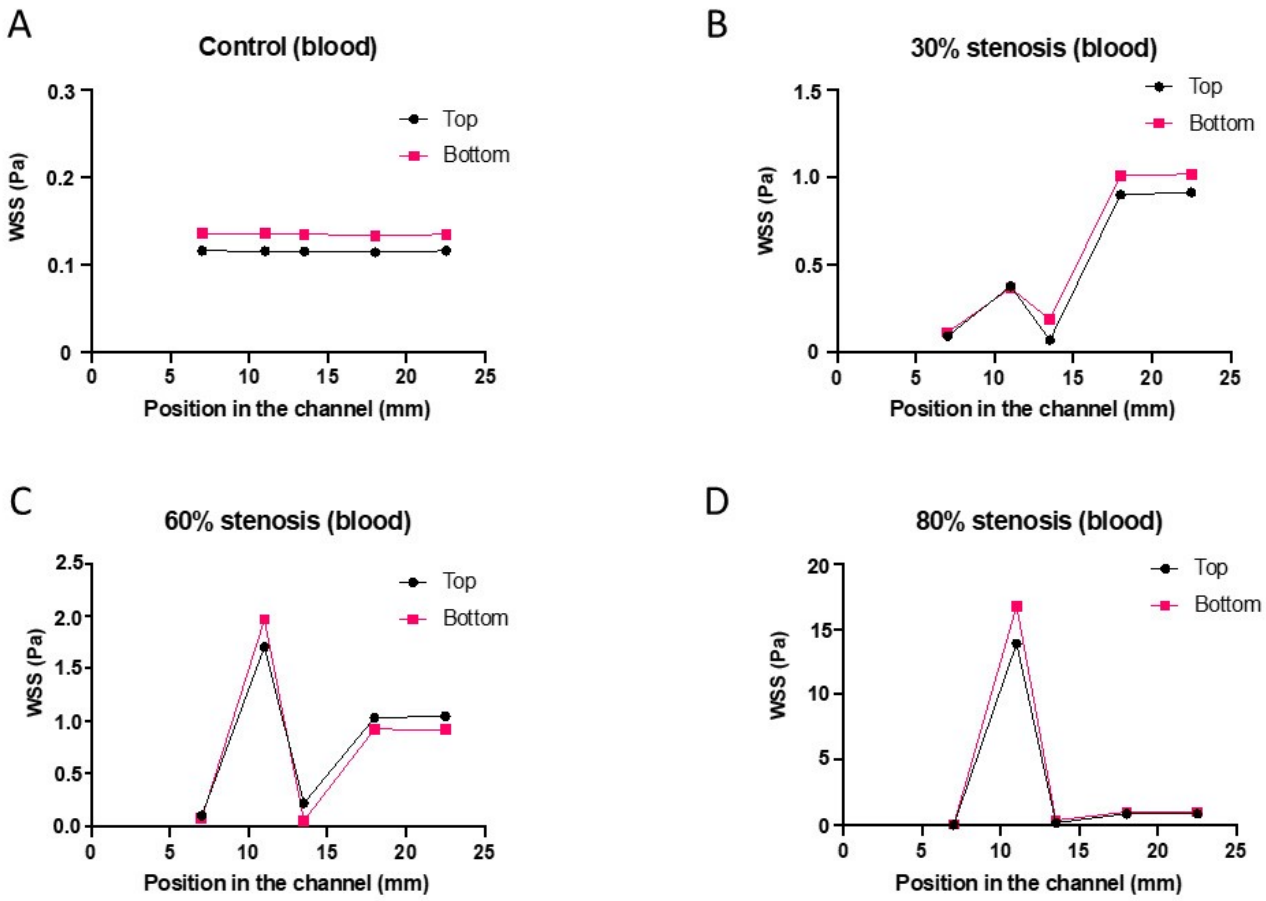


**Figure S20. Wall shear stress values at the top and bottom regions of semi-circular channels, for simulations run with blood.** Wall shear stress (WSS) values at the top and bottom regions of the channels in the control (A), 30% (B), 60% (C) and 80% (D) stenosis models, for simulations run with blood. The X axis indicates the different regions of the channel: upstream (7 mm), stenosis (11 mm), post-stenotic dilatation (13.5 mm), downstream 1 (18 mm) and downstream 2 (22.5 mm). All simulations were performed in CFX (Ansys, Inc.), using an inlet velocity of 20mm/sec (0.17 L/h) and outlet pressure of 1.16 kPa.

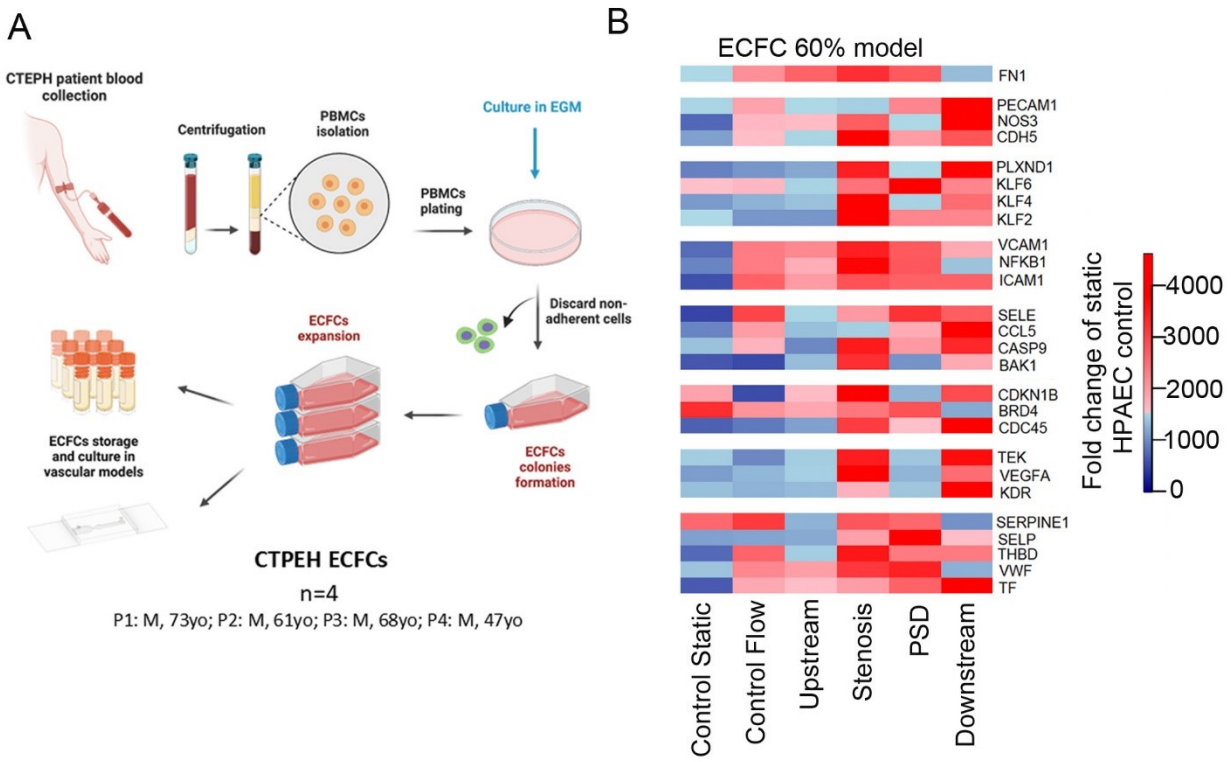


**Supplementary Figure S21. Changes in gene expression in CTEPH endothelial colony forming cells (ECFCs) cultured in 60% model. (A)** Isolation of ECFCs. **(B)** Expression of marker genes of thrombosis, inflammation, angiogenesis, proliferation, and stimulation by flow was measured in CTEPH-derived endothelial colony forming cells (ECFCs) cultured in the 60% stenosis model and exposed to flow for 6h, and pulmonary endarterectomy (PEA) cells. The heatmap shows the fold change of gene expression, relative to human pulmonary artery endothelial cells (HPAECs) (control static). The heatmap was generated using R 4.3.3 (The R Project for Statistical Computing, 2024). PSD: post-stenotic dilatation.

**SUPPLEMENTARY TABLES**

Salina Nicoleau et al. 3D Modelling of Pulmonary Arterial Geometry and Endothelial Dysfunction in CTEPH

| Patient | Occlusion (%) | Mean occlusion (%) |
|---|---|---|
| **CTEPH 1** | 47.18 | 49.77 |
| | 52.37 | |
| **CTEPH 2** | 52.08 | 49.94 |
| | 47.79 | |
| **CTEPH 3** | 45.29 | 65.05 |
| | 84.81 | |
| **CTEPH 4** | 64.01 | 63.11 |
| | 62.22 | |
| **CTEPH 5** | 41.65 | 43.08 |
| | 48.89 | |
| | 38.70 | |
| **CTEPH 6** | 49.63 | 48.72 |
| | 47.81 | |
| **CTEPH 7** | 20.84 | 25.97 |
| | 22.32 | |
| | 34.74 | |

**Table S1. CT-scan derived measurements of pulmonary arterial stenosis in CTEPH patients**
Measurements were taken from computed tomography scans from CTEPH patients (n=7) using the "measure" function in Mimics 23.0 (Materialise, 2021). Occlusion % were calculated as [(1-luminal diameter)/pulmonary arterial diameter]x100.

| Publication | Artery diameter | Degree of obstruction | Study type | Number of patients | Notes |
|---|---|---|---|---|---|
| **Moser et al, 1993** | 25-100 µm | 54.5 (%ED) | Lung specimens | 5 | |
| | | 72.3 (%ED) | | | |
| | | 77.6 (%ED) | | | |
| | | 64.3 (%ED) | | | |
| | | 57.1 (%ED) | | | |
| **Sanda et al, 2019** | 170.3 ± 59.8 µm | 85 ± 13.9 % | Lung specimens | 33 | Deduced from mean obstruction ratio ( [(intimal area/vascular area of PAs) + ( medial |
| **Azarian et al, 1997** | N/A | 58 ± 15 % (PVO) | Perfusion lung scans | 45 | PVO: see full article for details |
| **Miniati et al, 2006** | All PAs | 59.7 % (52.3 - 74.5%) (PVO) | Perfusion lung scans | 4 | PVO = (1- overall perfusion score) x 100 |
| **Kawakami et al, 2016** | 3.9 mm | 58% | Perfusion lung scans | 1 | |
| **Spazzapan et al, 2018** | LPA | 40.3% | CFD modelling (based on patient morphometrics) | 1 | |
| | LPA | 37.3% | | 1 | |
| | RPA | 43.8% | | 1 | |
| | LPA | 71.5% | CFD modelling | N/A | Used to model severe case of CTEPH but not based on patient morphometrics |

**Table S2. Literature-derived measurements of pulmonary arterial stenosis in CTEPH patients**
CFD: computational fluid dynamics; CTPEH: chronic thromboembolic pulmonary hypertension; ED: external diameter (of the pulmonary artery); PA: pulmonary artery; PVO: pulmonary vascular obstruction.

| Model | Fluid | Inlet flow rate (L/h) | Inlet velocity (mm/sec) | Tubing inner diameter (mm) | Outlet pressure (kPa) | Reynolds |
|---|---|---|---|---|---|---|
| Semi-circular | Water | 0.50 | 60.2 | 2.79 | 0.097 | 255 |
| | Blood | 0.17 | 20 | 1.60 | 1.16 | 21 |
| Fully circular | Water | 2.26 | 50 | 2.00 | 1.60 | 212 |
| | Blood | 0.68 | 15 | 2.00 | 1.92 | 16 |

**Table S3. Inlet and outlet boundary parameters used for the CFD simulations in circular and semi-circular models**. Inlet velocity of 157mm/sec (1.31L/h) and outlet pressure of 2.94kPa were used for the mesh convergence analyses (run with water).

| Mesh | Element size | | | |
|---|---|---|---|---|
| | Fluid | Inlet | Outlet | Wall |
| **M1** | 0.6 | 0.4 | 0.4 | 0.4 |
| **M1.5** | 0.45 | 0.3 | 0.3 | 0.3 |
| **M2** | 0.3 | 0.2 | 0.2 | 0.2 |
| **M2.5** | 0.25 | 0.15 | 0.15 | 0.15 |
| **M3.5** | 0.2 | 0.1 | 0.1 | 0.1 |
| **M3.5** | 0.15 | 0.08 | 0.08 | 0.08 |
| **M4** | 0.12 | 0.07 | 0.07 | 0.07 |

**Table S4 Part element sizes used for each mesh used in the convergence analysis**
Each mesh was generated in ICEM CFD (Ansys, Inc.).

| | Total number of elements | | | | | | |
|---|---|---|---|---|---|---|---|
| | M1 | M1.5 | M2 | M2.5 | M3 | M3.5 | M4 |
| **Control** | 45175 | 82975 | 171335 | 366312 | 764489 | 1227287 | - |
| **30% stenosis** | 32838 | 58198 | 148606 | 248440 | 652096 | 930232 | - |
| **60% stenosis** | 32590 | 55682 | 131532 | 248347 | 564194 | 1009869 | - |
| **80% stenosis** | 30571 | 53208 | 141954 | 228748 | 546233 | 864234 | 1147812 |

**Table S5 Total number of elements for each mesh used in the convergence analysis**
M1-M4: Mesh 1 to Mesh 4; around 2-fold increase in element size between each mesh. Each mesh was generated in ICEM CFD (Ansys, Inc.).

| CONTROL | Mean WSS (dyn/cm2) | | | | |
|---|---|---|---|---|---|
| Mesh | M1.5 | M2 | M2.5 | M3 | M3.5 |
| Pre-stenosis (7mm) | 2.31 | 2.48 | 2.71 | 2.77 | 2.70 |
| Stenosis apex (11mm) | 2.29 | 2.44 | 2.69 | 2.66 | 2.75 |
| Dilatation apex (13.5mm) | 2.41 | 2.53 | 2.65 | 2.65 | 2.64 |
| Post-stenosis 1 (18mm) | 2.38 | 2.55 | 2.54 | 2.63 | 2.46 |
| Post-stenosis 2 (22.5mm) | 2.49 | 2.65 | 2.60 | 2.72 | 2.52 |
| % difference | %D M2/1.5 | %D M2.5/2 | %D M3/2.5 | %D M3.5/3 | - |
| Pre-stenosis (7mm) | 7.34 | 8.90 | 2.22 | 2.64 | |
| Stenosis apex (11mm) | 6.29 | 9.76 | 1.31 | 3.48 | |
| Dilatation apex (13.5mm) | 4.85 | 4.75 | 0.30 | 0.09 | |
| Post-stenosis 1 (18mm) | 7.00 | 0.53 | 3.68 | 6.93 | |
| Post-stenosis 2 (22.5mm) | 6.25 | 2.21 | 4.74 | 7.59 | |
| Average % difference | 6.347 | 5.229 | 2.449 | 4.145 | |

**Table S6. Mean WSS and percentage difference in WSS value between meshes in each region of the control channel.** M1-M3.5: Mesh 1 to Mesh 3.5; around 2-fold increase in element size between each mesh. WSS: wall shear stress; 1 dyne/cm$^2$ =0.1Pa. Each mesh was generated in ICEM CFD (Ansys, Inc.) and all simulations were performed in CFX (Ansys, Inc.).

| 30% STENOSIS | Mean WSS (dyn/cm2) | | | | |
|---|---|---|---|---|---|
| Mesh | M1.5 | M2 | M2.5 | M3 | M3.5 |
| Pre-stenosis (7mm) | 1.83 | 2.11 | 2.22 | 2.36 | 2.38 |
| Stenosis apex (11mm) | 7.27 | 9.44 | 9.49 | 10.00 | 10.10 |
| Dilatation apex (13.5mm) | 2.73 | 2.97 | 3.11 | 3.36 | 3.45 |
| Post-stenosis 1 (18mm) | 18.29 | 17.99 | 18.71 | 19.48 | 19.72 |
| Post-stenosis 2 (22.5mm) | 17.59 | 18.64 | 20.22 | 21.29 | 21.20 |
| % difference | %D M2/1.5 | %D M2.5/2 | %D M3/2.5 | %D M3.5/3 | - |
| Pre-stenosis (7mm) | 14.25 | 5.19 | 6.15 | 0.76 | |
| Stenosis apex (11mm) | 25.98 | 0.57 | 5.20 | 1.05 | |
| Dilatation apex (13.5mm) | 8.33 | 4.50 | 7.73 | 2.72 | |
| Post-stenosis 1 (18mm) | 1.62 | 3.92 | 4.03 | 1.21 | |
| Post-stenosis 2 (22.5mm) | 5.78 | 8.16 | 5.13 | 0.40 | |
| Average % difference | 11.191 | 4.469 | 5.646 | 1.227 | |

**Table S7. Mean WSS and percentage difference in WSS value between meshes in each region of the 30% stenosis channel.** M1-M3.5: Mesh 1 to Mesh 3.5; around 2-fold increase in element size between each mesh. WSS: wall shear stress; 1 dyne/cm$^2$ =0.1Pa. Each mesh was generated in ICEM CFD (Ansys, Inc.) and all simulations were performed in CFX (Ansys, Inc.).

| 60% STENOSIS | Mean WSS (dyn/cm2) | | | | |
|---|---|---|---|---|---|
| **Mesh** | **M1.5** | **M2** | **M2.5** | **M3** | **M3.5** |
| **Pre-stenosis (7mm)** | 1.63 | 1.86 | 1.94 | 2.13 | 2.10 |
| **Stenosis apex (11mm)** | 45.42 | 48.12 | 57.89 | 59.93 | 60.83 |
| **Dilatation apex (13.5mm)** | 9.89 | 9.84 | 12.03 | 14.26 | 13.80 |
| **Post-stenosis 1 (18mm)** | 15.08 | 15.71 | 18.52 | 20.02 | 20.21 |
| **Post-stenosis 2 (22.5mm)** | 17.55 | 17.98 | 20.87 | 22.39 | 22.44 |
| **% difference** | **%D M2/1.5** | **%D M2.5/2** | **%D M3/2.5** | **%D M3.5/3** | - |
| **Pre-stenosis (7mm)** | 13.34 | 3.92 | 9.53 | 1.64 | |
| **Stenosis apex (11mm)** | 5.76 | 18.43 | 3.46 | 1.49 | |
| **Dilatation apex (13.5mm)** | 0.51 | 19.99 | 17.01 | 3.27 | |
| **Post-stenosis 1 (18mm)** | 4.08 | 16.40 | 7.81 | 0.95 | |
| **Post-stenosis 2 (22.5mm)** | 2.39 | 14.91 | 7.01 | 0.21 | |
| **Average % difference** | 5.216 | 14.731 | 8.965 | 1.512 | |

**Table S8. Mean WSS and percentage difference in WSS value between meshes in each region of the 60% stenosis channel.** M1-M3.5: Mesh 1 to Mesh 3.5; around 2-fold increase in element size between each mesh. WSS: wall shear stress; 1 dyne/cm$^2$ =0.1Pa. Each mesh was generated in ICEM CFD (Ansys, Inc.) and all simulations were performed in CFX (Ansys, Inc.).

| 80% STENOSIS | Mean WSS (dyn/cm2) | | | | | |
|---|---|---|---|---|---|---|
| Mesh | M1.5 | M2 | M2.5 | M3 | M3.5 | M4 |
| Pre-stenosis (7mm) | 1.65 | 1.98 | 1.93 | 2.06 | 2.06 | 2.06 |
| Stenosis apex (11mm) | 1043.27 | 132.11 | 607.87 | 496.34 | 585.02 | 588.63 |
| Dilatation apex (13.5mm) | 23.35 | 36.42 | 43.35 | 64.44 | 93.41 | 94.27 |
| Post-stenosis 1 (18mm) | 13.50 | 19.49 | 14.63 | 17.52 | 32.70 | 34.91 |
| Post-stenosis 2 (22.5mm) | 15.96 | 16.54 | 19.51 | 18.75 | 25.13 | 24.91 |
| % difference | %D M2/1.5 | %D M2.5/2 | %D M3/2.5 | %D M3.5/3 | %D M4/M3.5 | - |
| Pre-stenosis (7mm) | 18.24 | 2.74 | 6.37 | 0.11 | 0.20 | |
| Stenosis apex (11mm) | 155.04 | 128.59 | 20.20 | 16.40 | 0.61 | |
| Dilatation apex (13.5mm) | 43.76 | 17.37 | 39.13 | 36.71 | 0.91 | |
| Post-stenosis 1 (18mm) | 36.33 | 28.51 | 18.01 | 60.45 | 6.53 | |
| Post-stenosis 2 (22.5mm) | 3.60 | 16.46 | 3.99 | 29.10 | 0.87 | |
| Average % difference | 51.393 | 38.731 | 17.540 | 28.555 | 1.828 | |

**Table S9. Mean WSS and percentage difference in WSS value between meshes in each region of the 80% stenosis channel**. M1-M4: Mesh 1 to Mesh 4; around 2-fold increase in element size between each mesh. WSS: wall shear stress; 1 dyne/cm$^2$ =0.1Pa. Each mesh was generated in ICEM CFD (Ansys, Inc.) and all simulations were performed in CFX (Ansys, Inc.)

| Sample type | Patent informa;on | Patent number | Corresponding colour of datapoints in graphs |
|---|---|---|---|
| ECFCs (CTEPH) | Male, 73 y.o. | 1 | Purple |
| ECFCs (CTEPH) | Male, 61 y.o. | 2 | Green |
| ECFCs (CTEPH) | Male, 68 y.o. | 3 | Blue |
| ECFCs (CTEPH) | Male, 47 y.o. | 4 | Magenta |
| PEA | Male, 73 y.o. | 1 | - |
| PEA | Male, 47 y.o. | 2 | - |
| ECFCs (healthy) | Female, 23 y.o. | 1 | - |
| ECFCs (healthy) | Female, 29 y.o. | 2 | - |
| ECFCs (healthy) | Female, 36 y.o. | 3 | - |

**Table S10. Donor characteristics.** Cells were kindly donated by Dr Olga Tura-Ceide, from the Hospital Clinic de Barcelona (Barcelona, Spain). ECFCs: endothelial colony forming cells; PEA: pulmonary endarterectomy.

| Component | **Volume added to make the 20uL reaction solution** | **Final concentration** |
|---|---|---|
| **LunaScript RT SuperMix (5x)** | 4µL | 1x |
| **RNA sample** | Variable | 50-200ng |
| **Nuclease-free water** | Remaining volume up to 20µL | - |

**Table S11 Details of the reverse transcription reaction mix**
No-RT Control Mix (5x) was used to make negative controls to check for DNA/RNA contaminations.

| **Cycle Step** | **Temperature** | **Time** | **Cycles** |
|---|---|---|---|
| Primer Annealing | 25 °C | 2 minutes | 1 |
| cDNA Synthesis | 55 °C | 10 minutes | 1 |
| Heat Inactivation | 95 °C | 1 minute | 1 |

**Table S12. Reverse transcription cycling conditions**
All samples were reverse transcribed using a SimpliAmpTM Thermal Cycler (Applied Biosystems, UK).

| Name | **Direction** | **Sequence (5' to 3')** |
|---|---|---|
| **TF** | Forward | CGGACAGCCAACAATTCAGAGTTT |
| | Reverse | GATGACCACAAATACCACAGCTCC |
| **THBD** | Forward | CCTTCCTCAATGCCAGTCAGATCT |
| | Reverse | GTTGTTGTCTCCCGTAACCCACTG |
| **SELP** | Forward | GGCATAGCATCACTTCCTACTCCA |
| | Reverse | TCCTATGAGTGTGAATCCAGCGTT |
| **CDC45** | Forward | CTGAAGCAGGTGAAGCAGAAGTTC |
| | Reverse | AGAGCCTGGATGAAGTGATCTGTC |
| **CASP9** | Forward | GCTCTTCCTTTGTTCATCTCCTGC |
| | Reverse | TCTGCATTTCCCCTCAAACTCTCA |
| **NFKB1** | Forward | TCCGTTATGTATGTGAAGGCCCAT |
| | Reverse | AGTTACAGTGCAGATCCCATCCTC |
| **CCL5** | Forward | CTCGCTGTCATCCTCATTGCTACT |
| | Reverse | AGTTGATGTACTCCCGAACCCATT |

| | | |
|---|---|---|
| **PLXND1** | Forward | GGCCATTCTGAGTATCCGTGAAGA |
| | Reverse | ATGTGGTCTGTCTTGTCGATGTCA |
| **KLF2** | Forward | GTGAGAAGCCCTACCACTGCAACT |
| | Reverse | CCGGTTCTCTGGGTCCAATAAATA |
| **KLF4** | Forward | TGGACCCCCTCTCAGCAATG |
| | Reverse | CTCTTGGTAATGGAGCGGCG |
| **KLF6** | Forward | AGCGTTAGTCACTGCTCATTTC |
| | Reverse | GGGTGTGGCTCTTTGCTTTA |
| **VEGFA** | Forward | AGGGAAAGGGGCAAAAACGAAAG |
| | Reverse | ACAAATGCTTTCTCCGCTCTG |
| **BAK1** | Forward | GCCACCAGCCTGTTTGAGAGT |
| | Reverse | GACCATTGCCCAAGTTCAGGG |
| **CDKN1B (p27)** | Forward | TGCGCAGGAATAAGGAAGCG |
| | Reverse | CGAGCTGTTTACGTTTGACGTCTT |
| **VCAM-1** | Forward | AAAATCGAGACCACCCCAGAATCT |
| | Reverse | ACAGGTAAGAGTGTTCGTTCCCAA |
| **PECAM-1 (CD31)** | Forward | TGGAAGGAGTGCCCAGTCCCA |
| | Reverse | CGGAAGGATAAAACGCGGTCCTG |
| **CDH5** | Forward | CCTCCGATACATGAGCCCTCC |
| | Reverse | TCGGAAGAACTGGCCCTTGT |
| **B2M** | Forward | CCAGCGTACTCCAAAGATTCAGG |
| | Reverse | TCAATGTCGGATGGATGAAACCC |
| **TEK (TIE-2)** | Forward | GCAACCAATATTTCCAAGCTCGGA |
| | Reverse | AATGTCACTAAGGGTCCAAGCAGT |
| **ICAM-1** | Forward | GGCCAGCTTATACACAAGAACCAG |
| | Reverse | GTGCCATCCTTTAGACACTTGAGC |
| **BRD4** | Forward | CGTCAAGCTGAACCTCCCTGATTA |
| | Reverse | ATGATCTCGGTTTCTTCTGTGGGT |

| | | |
|---|---|---|
| **KDR** | Forward | CACCAGAAATGTACCAGACCATGC |
| | Reverse | AGTCCAGAATCCTCTTCCATGCTC |
| **E-SELECTIN** | Forward | CTGGGCTCCAGGTGAACCCAAC |
| | Reverse | CCGTGGCCACTGCAGGATGTA |
| **SERPINE1** | Forward | CCACAAATCAGACGGCAGCA |
| | Reverse | GGGCGTGGTGAACTCAGTATAGT |
| **VWF** | Forward | ATGTGGCGTTCGTCCTGGAA |
| | Reverse | TTGGACTGTGCCTCGCTGAA |
| **NOS3** | Forward | ATCCCCCGGAGAATGGAGAG |
| | Reverse | AGCGGATCTTATAACTCTTGTGCT |
| **Fibronectin** | Forward | GGCCCCATTCCAGGACACTT |
| | Reverse | TTGACAGAGTTGCCCACGGT |

**Table S13. qPCR primer sequences used for each gene of interest**

| Component | 10µL Reaction | Final Concentration |
|---|---|---|
| Luna Universal qPCR Master Mix | 5 µL | 1X |
| 10 µM forward primer | 0.5 µL | 0.25 µM |
| 10 µM reverse primer | 0.5 µL | 0.25 µM |
| Nuclease-free water | 3 µL | - |
| cDNA products | 1 µL | 1 ng |

**Table S14. Components used in the qPCR reactions**

| Cycle Stage | Temperature | Time | Cycles |
|---|---|---|---|
| **Hold Stage** | 50 °C | 2 minutes | 1 |
| | 95 °C | 5 minutes | |
| **PCR Stage** | 95 °C | 15 seconds | 40 |
| | 62 °C | 30 seconds | |
| **Melt Curve Stage** | 95 °C | 15 seconds | 1 |
| | 60 °C | 1 minute | |
| | 95 °C | 15 seconds | |

**Table S15. qPCR amplification cycles and cycling conditions**
All qPCR amplifications were performed with a QuantStudio 12K Flex Real-Time PCR System (Applied Biosystems, USA).